


## Synthesis of silver nanoparticles: double-green approach of using chitosan and microwave technique towards antimicrobial activity against pathogenic bacteria

Alyza A. Azmi <sup>1,\*</sup> , Norhidayah Ahyat <sup>1</sup>, Faridah Mohamad <sup>1</sup>, Sofiah Hamzah <sup>2</sup>

<sup>1</sup>Faculty of Science and Marine Environment, Universiti Malaysia Terengganu, 21030 Kuala Nerus, Terengganu, Malaysia

<sup>2</sup>Faculty of Ocean Engineering, Technology and Informatics, Universiti Malaysia Terengganu, 21030 Kuala Nerus, Terengganu, Malaysia

\*corresponding author e-mail address: [alyza.azzura@umt.edu.my](mailto:alyza.azzura@umt.edu.my) | Scopus ID [55023192300](https://orcid.org/0000-0001-9230-5502)

### ABSTRACT

A double green approach to the synthesis of silver nanoparticles using chitosan as a reducing agent and microwave radiation has been carried out in this study. Chitosan was extracted from marine crab carapace and the morphology of the produced chitosan was characterized using Scanning Electron Microscope (SEM). The production of silver nanoparticles (AgNPs) was monitored by the formation of surface plasmon resonance (SPR) at the  $\lambda_{\text{max}} = 420$  nm, indicates the reduction of the oxidation state of  $\text{Ag}^+$  to  $\text{Ag}^0$ . The XRD data confirms the crystallinity nature of obtained AgNPs, while the SEM and TEM revealed the formation of near-spherical shapes, polydisperse, heterogeneous distribution of AgNPs with the size range between 7 to 25 nm. The antimicrobial activities of the AgNPs were investigated using The prepared AgNPs demonstrated dual mechanism action with chitosan, which acted as a stabilizer on the surface of AgNPs, and enhance the inhibition zone against *E. tarda* and *E. coli*. Therefore, the synthesized AgNPs in this study may have excellent potential for clinical application as it is green, low-cost and eco-friendly.

**Keywords:** green; silver nanoparticles; chitosan; microwave; antimicrobial activity.

### 1. INTRODUCTION

The development of metallic nanoparticles has gained tremendous interest due to their novel chemical and physical properties that differ from their bulk counterparts. Metal nanoparticles have a large surface area per volume unit that can practically apply in many areas such as cosmetics, medicine, food processing and energy [1-2]. Specifically, the development of silver nanoparticles (AgNPs) has raised exponentially due to the ability of the nanoparticles to penetrate the wall of microbial cells and enhances their application as antimicrobial agents [3-6]. Therefore, dealing with nanoparticles that have high therapeutic properties, there is a growing need to produce the AgNPs in a 'greener' way to circumvent the adverse by-product from the synthesis.

The green method receives considerable attention in the preparation of AgNPs as it is promoting a clean, rapid, simple and non-toxic approach. The replacement of hazardous and toxic reducing agents with eco-friendly materials has been explored extensively. For instance, the biological system including plant extracts, animal cell cultures, and microorganisms is an alternative procedure for the preparation of the AgNPs. In the most recent studies, utilization of *Coriandrum Sativum* leaf extract [7], Thermophilic *Bacillus Sp.* AZ1 [8], plant extract of *Lampranthus*

*coccineus* and *Malephora lutea* [9], marine algae *Caulerpa racemose* [10], and yeast extract [11] as reducing and capping agent in the biosynthesis of AgNPs were investigated extensively. It was also reported that the produced AgNPs is an effective biocidal agent against a wide range of Gram-negative and Gram-positive bacteria, as well as multidrug-resistant bacteria and fungal pathogens.

In the present work, we aimed to prepared AgNPs using chitosan. Chitosan is a polysaccharide produced from chitin derivation and widely distributes in the exoskeleton of marine invertebrates, insects, arthropods or mollusks [12-13]. Chitosan is also known as a polycationic biopolymer that consists of large free amino and hydroxyl groups, which is responsible to reduce metal salt into metal nanoparticles. Additionally, chitosan is a renewable, biodegradable and non-toxic product that may lead to the sustainable development of the AgNPs

Herein, we reported a simple, rapid and clean synthesis of novel AgNPs using chitosan extracted from the carapace of marine crabs as reducing agents *via* microwave-aided radiation heat techniques and their influence against *Edwardsiella tarda* and *Escherichia coli*.

### 2. MATERIALS AND METHODS

#### 2.1. Chitosan extraction.

The extraction of chitosan from the carapace of marine crabs (*Portunus pelagicus*) was published by Norhidayah et al. (2017) [14]. The chitosan extraction involves four steps, which are demineralization, deproteinization, decolorization, and deacetylation. the functional groups of the obtained chitosan powder were confirmed using FTIR (Perkin Elmer Spectrum 100 FT-IR Spectrometer) in the transmission mode using KBr support. Thermogravimetric analysis (Perkin Elmer TGA analyzer) were

carried out using approximately 10 mg of the sample with a temperature range of 30 – 600 °C, while the crystallinity nature of the chitosan was examined using XRD analysis (Rigaku MiniFlex II) equipped with Ni – filtered Cu K $\alpha$  radiation ( $\lambda = 1.5406$  Å) as the X-ray source. The dry weight of chitosan content was calculated to be at 13.56%.

Chitosan suspension was prepared by dissolving 0.5 g chitosan in 100 mL of acetic acid (2 % v/v) solution. The mixture was stirred until a homogenous solution was obtained. The mixture

## Synthesis of silver nanoparticles: double-green approach of using chitosan and microwave technique towards potential antimicrobial activity against pathogenic bacteria

of chitosan and AgNO<sub>3</sub> suspension at different concentrations (0.1 M, 0.2 M, and 0.3 M) was heated in a microwave oven (Panasonic NN-GD371M Microwave Oven) for 4 minutes with output power fixed at 950 W. The formation of Ag nanoparticles was indicated by the change of the color from light yellow to dark brown. The produced AgNPs were collected by centrifugation at 15,000 rpm for 15 minutes.

### 2.3. Characterization of AgNPs.

The formation of the AgNPs synthesized using chitosan was monitored using UV-Visible absorption (UV-1800 Spectrophotometer Shimadzu) from 300 to 600 nm. The AgNPs characteristic plasmon absorption band was observed at a range of 380 to 450 nm. The crystallinity of the AgNPs produced was observed using an X-ray diffractometer (Rigaku MiniFlex II). The peak intensity for the Ag Nps was collected in the 2θ range 20° to

80° and the scanning speed at 0.5 min per degree. The morphology of the synthesized AgNPs was performed using Energy Filtered Transmission Electron Microscopy (EFTEM, LIBRA 120), at an accelerating voltage of 120 kV.

### 2.4. Antibacterial activity.

The antimicrobial activity of AgNPs was measured from the zone of inhibition using agar well diffusion method against *Edwardsiella tarda* (*E. tarda*) and *Escherichia coli* (*E. coli*). Muller Hinton Agar plates were swabbed with fresh bacteria cultures (10<sup>8</sup> CFU/mL) using a sterile cotton swab. Holes were made using sterile cork borer and filled with AgNPs. Chitosan solution extracted from the carapace of marine crabs were served as negative control and oxytetracycline (the antibiotic) were served as a positive control. The diameter of inhibition zones was measured recorded and assessed qualitatively after 24 hours of incubation.

## 3. RESULTS

### 3.1. Chitosan extraction.

The yield of chitin and chitosan was obtained by comparing the weight of the material to the weight of chitin or chitosan. The percentage of weight loss obtained during demineralization, deproteinization, decolorization and deacetylation processes from the marine crab shell was tabulated in Table 1. The demineralization process shows the highest weight loss of the sample (78.8%), which contributes to the inorganic material removal. The addition of the acidic solution to the calcium carbonate (CaCO<sub>3</sub>) resulted in the formation of solid calcium chloride, and the emission of CO<sub>2</sub> gas [15]. The removal of protein and color pigments was conducted in the second and third stages with the percentage weight loss of 16.03 and 6.74%, respectively.

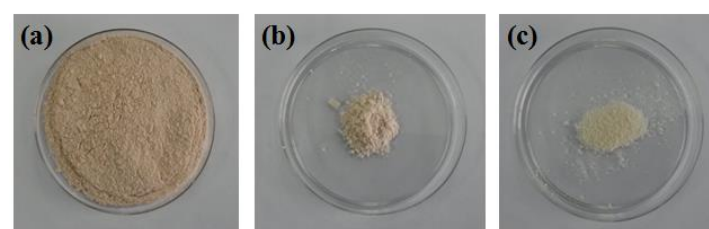


Figure 1. The photograph of prepared samples of the marine crab shell a) raw powder, b) chitin, c) chitosan.

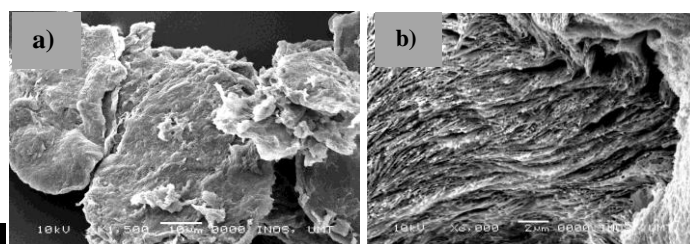


Figure 2. SEM micrograph of a) chitin and b) chitosan extracted from marine crab shells.

Table 1. Percentage of weight loss of the marine crab shell at each extraction process.

Process	Initial Weight (g)	Weight after treatment (g)	Weight loss (%)
Demineralization	10.0	2.12	78.80
Deproteinization	2.12	1.78	16.03
Decolourization	1.78	1.66	6.74
Deacetylation	1.66	1.55	6.63

The color of the raw powder was changed from light brown to white as depicted in figure 1, which indicates the potential of chitosan formation. SEM micrographs of chitin and chitosan samples synthesis from marine crab shells are shown in figure 2. The SEM image of the chitin sample indicates the presence of diverse shapes (figure 2a), with appreciable voids on their surface. The formation of voids shows the successful removal of CaCO<sub>3</sub> by acid treatment in the demineralization process, leaving holes with irregular shapes. The formation of the fibrous structure was revealed in higher magnification of the SEM image of the deacetylated sample (figure 2b). This result supports the amorphous nature of chitosan powder, which obtained by XRD analysis [14]. All samples of the chitosan powder produced in this study exhibited similar morphological behavior. The detailed physicochemical characteristic of the chitosan extracted from marine crab carapace is published by Norhidayah et al. (2017) [14].

### 3.2. Formation of AgNPs.

The formation of AgNPs was preliminarily confirmed by the of the solutions from colorless to brown (inset figure 3). Figure 3 shows the UV-Vis spectra of AgNPs produced by microwave radiation after 4 minutes of reaction. The symmetrical band with a maximum curve peak at 410 nm for freshly prepared AgNPs indicates the excitation of surface plasmon resonance (SPR) electrons [10, 16]. The SPR becomes the indicator to determine the reduction of silver ions (Ag<sup>+</sup>) by chitosan in the solution into the AgNPs (Ag<sup>0</sup>). The absorption intensity SPR band also shows an increasing trend as the concentration of AgNO<sub>3</sub> solution increased, consistent with the color change of the solution, from yellow to dark brown (inset figure 3). For the determination of AgNPs stability, the samples have been stored for 6 months, and UV-Vis absorption spectra were recorded again. There is no major difference shown in the UV-Vis spectra in figure 4, indicates that the AgNPs are stable without agglomeration. Thus, chitosan was successfully acted as a reducing agent and stabilizer on the surface of AgNPs that prevent aggregation process.

The 0.2 M concentration of AgNO<sub>3</sub> was chosen as an optimum condition for further analysis.

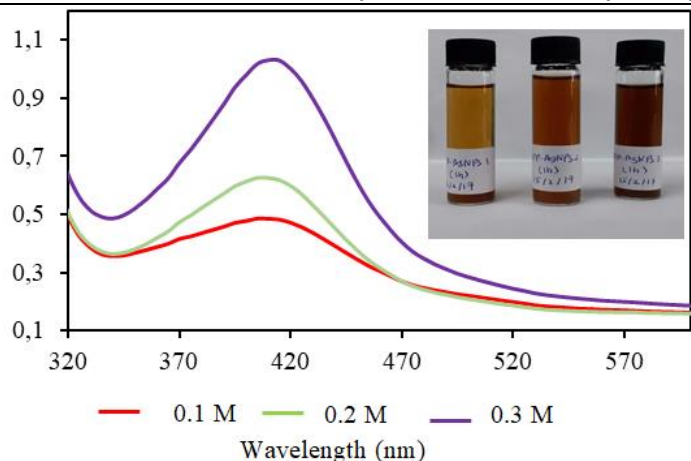


**Figure 3.** UV-Vis spectra of the synthesized AgNPs using chitosan from marine crab shells.

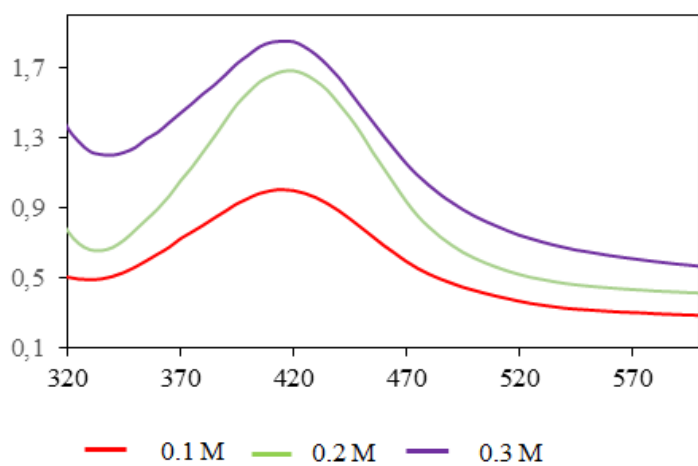


**Figure 4.** UV-Vis spectra of the synthesized AgNPs after 6 months of storage.

The diffraction data for the obtained AgNPs was recorded and the XRD pattern in figure 5 designate the crystalline nature of the AgNPs. Four different peaks were assigned to (111), (200), (220), and (311) planes of face cubic centered at  $2\theta$  values. This diffraction pattern is consistent with the previous research reported (Joseph and Mathew, 2015).

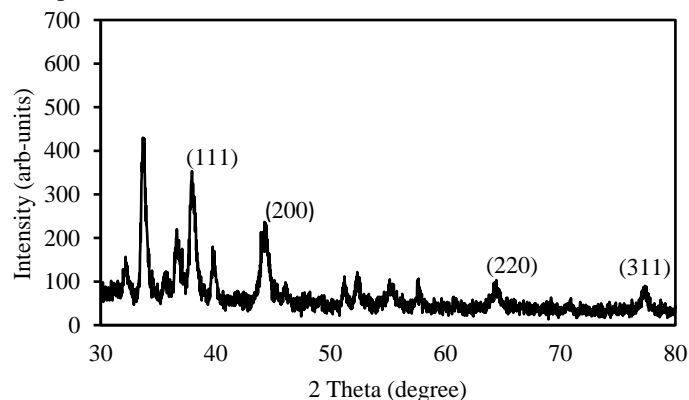


**Figure 5.** X-ray diffraction patterns of the synthesized AgNPs.

The intensity of the peak due to the reflection from (111) Bragg's plane is higher than that of other planes due to the preferential adsorption of Ag atoms on (111) plane during crystal growth. The average crystalline size of the obtained AgNPs was estimated using Debye-Scherrer's equation:

$$D = \frac{0.9 \lambda}{\beta \cos \theta}$$

The width of (111) Bragg's reflection was determined, and the estimated average size of the AgNPs was calculated to be 17 nm. The unassigned peaks can be attributed to AgNO<sub>3</sub> residual, consistent with the finding reported by Oryan et al. (2018) [17].

The SEM and transmission electron micrographs of the synthesized AgNPs are shown in figure 6. The SEM image (figure 6a) reveals the formation of polydisperse and heterogeneous distribution of AgNPs. The result was confirmed by the TEM image (figure 6b), which shows near-spherical shapes of AgNPs with the size range between 7-25 nm. The graph of the particle size distribution (figure 6c) also supports a narrow size distribution, and the synthesized AgNPs were stable without any aggregation after 6 months of storage as shown in figure 6d.

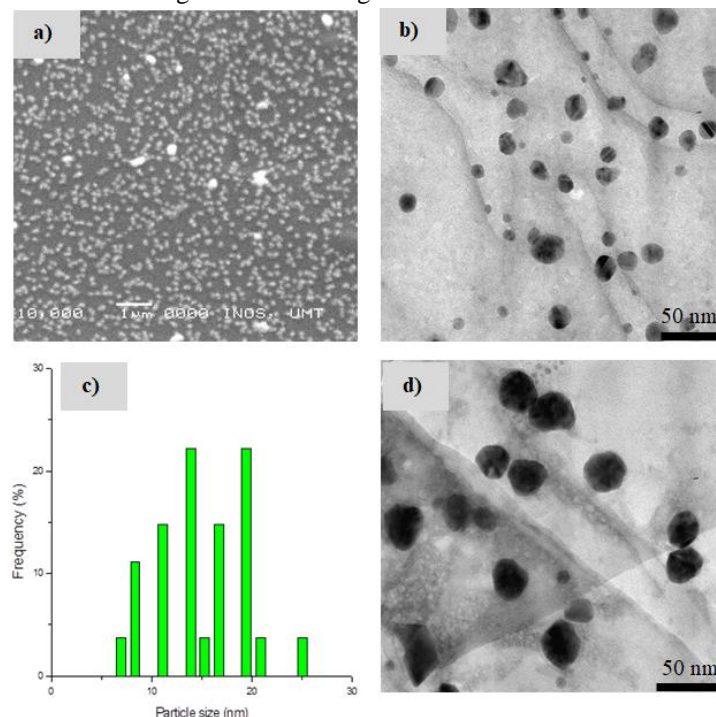


**Figure 6.** a) SEM image of synthesized AgNPs, b) TEM image of freshly prepared AgNPs, c) particle size distribution and d) TEM image of the AgNPs after 6 months of storage.

### 3.3 Antibacterial activity

Figure 7a and 7b show the effective inhibition zone of chitosan-capped AgNPs with the highest inhibition zone (diameter = 1.83 cm and 1.38 cm) towards *E. tarda* and *E.coli*, respectively.

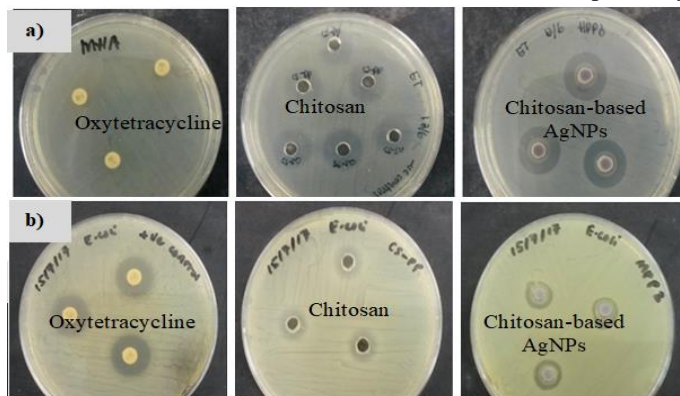


**Figure 7.** Antimicrobial activities of the AgNPs against a) *E.tarda* and b) *E.coli*.

The chitosan solution prepared from the marine crab shows a maximum zone of inhibition noted was 1.47 cm for *E.tarda*, while a diameter of 1.25 cm was observed in the case of *E.coli*. The antibiotic did not show any inhibition zone against *E. tarda* as it is

resistant towards oxytetracycline. In contrast, it can inhibit the growth of *E. coli* with a diameter of 1.70 cm of inhibition zone.

Table 2 summarized the data on the inhibition zone for the respective study.

**Table 2.** Tabulation of the maximum zone of inhibition.

Bacterial strain	Inhibition zone (cm)	
	<i>E. tarda</i>	<i>E. coli</i>
Oxytetracycline	0	1.70
Chitosan from marine crab	1.47	1.25
Ag nanoparticles using chitosan	1.77	1.38

Chitosan shows antimicrobial activity due to the cationic properties that contribute to the presence of amino functional groups in their backbone structure [18, 19]. The electrostatic

interaction between negatively charged microbial cell membranes and protonated  $\text{NH}_3^+$  groups of chitosan molecules causes a membrane disrupting effect and finally leading to cell death. The mechanism of inhibitory action of silver ions on microorganisms is well documented [3, 5, 20, 21]. It is believed that the mechanism of bactericidal actions of AgNPs is similar to the silver ions, where AgNPs and constituents of the bacterial membrane caused structural changes, inhibit respiratory enzymes, facilitating the generation of reactive oxygen species and consequently damaging the cell. Thus, the combination of chitosan and AgNPs is resulting in the highest microbial effect due to the dual mechanism of action between chitosan and AgNPs [22].

#### 4. CONCLUSIONS

The AgNPs reduced by chitosan extracted from the marine crab carapace (*Portunus pelagicus*) were successfully produced in an ecofriendly, inexpensive and efficient manner. The physicochemical properties of extracted chitosan were analyzed using spectroscopic and microscopic techniques and the obtained AgNPs were stable for up to 6 months of storage under ambient condition. Spherical shapes of the chitosan-based AgNPs were produced, with narrow size distribution, in the range of 7 to 25 nm. There is no evidence of agglomeration of colloidal nanoparticles

was observed during the 6 months of storage indicates high stability of AgNPs capped with chitosan. The produced AgNPs also have a clearer and higher inhibition zone towards *E. tarda* and *E. coli*. This finding demonstrated that the synthesized AgNPs using chitosan as reducing and stabilizing agents exhibits a dual mechanism of action to inhibit the growth of microorganisms, and thus presenting favorable characteristic for potential clinical application.

#### 5. REFERENCES

- Ibrahim, K.; Khalid, S.; Idrees, K. Nanoparticles: Properties, applications and toxicities. *Arab. J. Chem.* **2019**, *12*, 908-931, <https://doi.org/10.1016/j.arabjc.2017.05.011>.
- Fozia, I.; Mohammad, S.I.; Muhammad, M.A.; Muhammad, Z.S.; Abid, Yasmeen, R.A. Glucosylated-mediated green synthesis of gold and silver nanoparticles and their phyto-toxicity study. *Carbohydr. Polym.* **2014**, *104*, 29–33, <https://doi.org/10.1016/j.carbpol.2014.01.002>.
- Narayanawamy, K.; Athimoolam, R.; Ayyavoo, J. Green Synthesis of Silver Nanoparticles Using Leaf Extracts of *Clitoria ternatea* and *Solanum nigrum* and Study of Its Antibacterial Effect against Common Nosocomial Pathogens. *Journal of Nanoscience* **2015**, *928204*, 1-8, <https://doi.org/10.1155/2015/928204>.
- Shakeel, A.; Saifullah, M.A.; Babu, L.S.; Saiqa, I. Green synthesis of silver nanoparticles using *Azadirachta indica* aqueous leaf extract. *J Radiat Res Appl Sci* **2016**, *9*, 1-7, <https://doi.org/10.1016/j.jrras.2015.06.006>.
- Saba, P.; Maryam, G.; Saeid, B. Green synthesis of silver nanoparticles using the plant extract of *Salvia spinosa* grown in vitro and their antibacterial activity assessment. *J. Nanostructure Chem.* **2019**, *9*, 1–9, <https://doi.org/10.1007/s40097-018-0291-4>.
- Alyza, A.A.; Norhidayah, M.A. Green Synthesis of Silver Nanoparticles Using Rhizome Extract of Galangal. *Alpinia galangal, Mal. J. Anal. Sci.* **2015**, *19*, 1187–1193.
- Khan, M.Z.H.; Tareq, F.K.; Hossen, M.A.; Roki, M.N.A.M. Green Synthesis and Characterization of Silver Nanoparticles Using Coriandrum Sativum Leaf Extract. *J. Eng. Sci. Technol.* **2018**, *13*, 158–166.
- Ali, D.; Samad, G. Green Extracellular Synthesis of the Silver Nanoparticles Using Thermophilic *Bacillus Sp.* AZ1 and its Antimicrobial Activity Against Several Human Pathogenetic Bacteria. *Iran J. Biotechnol.* **2016**, *4*, 25–32. <https://dx.doi.org/10.15171/ijb.1259>.
- Eman, G.H.; Ali, M.E.; Mohamed, A.R.; Nagwan, M.G.; Mohamed, S.; Khayrya, A.Y.; Ahmed, S.; Abdullatif,

- B.M.; Abdulrhman, A.; Usama, R.A. Antiviral potential of green synthesized silver nanoparticles of *Lampranthus coccineus* and *Malephora lutea*. *Int. J. Nanomedicine* **2019**, *14*, 6217–6229, <https://doi.org/10.2147/IJN.S214171>.
- Kathiraven, T.; Sundaramanickam, A.; Shanmugam, N.; Balasubramanian, T. Green synthesis of silver nanoparticles using marine algae *Caulerpa racemosa* and their antibacterial activity against some human pathogens, *Appl Nanosci.* **2015**, *5*, 499–504, <https://doi.org/10.1007/s13204-014-0341-2>.
- Mengjun, S.; Fengjiao, H.; Zhaohui, Li.; Xingzhong, Z.; Yujie, M.; Zhihua, Z.; Zhi, Y.; Feng, G.; Min, Z. Biosynthesis and Antibacterial Activity of Silver Nanoparticles Using Yeast Extract as Reducing and Capping Agents. *Nanoscale Res Lett.* **2020**, *15*, 1-9, <https://doi.org/10.1186/s11671-019-3244-z>.
- Radwan, M.A.; Samia, F.A.; Abu-Elamayem, M.; Ahmed, N.S. Extraction, Characterization and Nematicidal Activity of Chitin and Chitosan Derived from Shrimp Shell Wastes. *Biol. Fertil. Soils.* **2012**, *28*, 463–468, <https://doi.org/10.1007/s00374-011-0632-7>.
- José, C. V. J.; Daylin, R. R.; Carlos, A. A.D.S.; Galba, M.D.C. Physicochemical and Antibacterial Properties of Chitosan Extracted from Waste Shrimp Shells. *Int. J. Microbiol.* **2016**, *5127515*, 1-7, <http://dx.doi.org/10.1155/2016/5127515>.
- Norhidayah, M. A.; Faridah, M.; Azrilawani, A.; Alyza, A. A. Chitin and Chitosan Extraction from *Portunus pelagicus*. *Mal. J. Anal. Sci.* **2017**, *21*, 770–777, <https://doi.org/10.17576/mjas-2017-2104-02>.
- Stephen, O.M. Current Development of Extraction, Characterization and Evaluation of Properties of Chitosan and Its Use in Medicine and Pharmaceutical Industry. *American Journal of Polymer Science* **2016**, *6*, 86-91.
- Ezzeldin, I.; Muchen, Z.; Yang, Z.; Afsana, H.; Wen, Q.; Yun, C.; Yanli, W.; Wenge, W.; Guochang, S.; Bin, L. Green-Synthesization of Silver Nanoparticles Using Endophytic Bacteria Isolated from Garlic and Its Antifungal Activity against Wheat Fusarium Head Blight Pathogen *Fusarium graminearum*,

*Nanomaterials* **2020**, *10*, 1-15,

<https://doi.org/10.3390/nano10020219>.

17. Ahmad, O.; Esmat, A.; Javad, T.; Sayedeh, F.N. A. Topical delivery of chitosan-capped silver nanoparticles speeds up healing in burn wounds: A preclinical study, *Carbohydr. Polym.* **2018**, *200*, 82-92, <https://doi.org/10.1016/j.carbpol.2018.07.077>.

18. Frank, L.A.; Onzi, G.R.; Morawski, A.S.; Pohlmann, A.R.; Guterres, S.S.; Contri, R.V. Chitosan as a coating material for nanoparticles intended for biomedical applications.

*React Funct Polym* **2020**, *147*,

<https://doi.org/10.1016/j.reactfunctpolym.2019.104459>.

19. Munawar, A.M.; Jaweria, T.M.S.; Kishor, M.W.; Ellen, K.W. An Overview of Chitosan Nanoparticles and Its Application in Non-Parenteral Drug Delivery. *Pharmaceutics* **2017**, *9*, 53-79,

<https://doi.org/10.3390/pharmaceutics9040053>.

20. Faizan, A.Q.; Anam, S.; Haris, M.K.; Fohad, M.H.; Rais, A.K.; Bader, A.; Ali, A.; Iqbal, A. Antibacterial Effect of Silver Nanoparticles Synthesized Using *Murraya koenigii* (L.) against Multidrug-Resistant Pathogens, *Bioinorg Chem Appl* **2019**, *4649506*, 1-11, <https://doi.org/10.1155/2019/4649506>.

21. Shijing, L.; Yapeng, Z.; Xuanhe, P.; Feizhou, Z.; Congyuan, J.; Qianqian, L.; Zhongyi, C.; Gan, D.; Guojun, W.; Linqian, W.; Liyu, C. Antibacterial activity and mechanism of silver nanoparticles against multidrug-resistant *Pseudomonas aeruginosa*. *Int. J. Nanomedicine* **2019**, *14*, 1469-1487, <https://doi.org/10.2147/IJN.S191340>.

22. Dongwei, W.; Wuyong, S.; Weiping, Q.; Yongzhong, Y.; Xiaoyuan, M. The synthesis of chitosan-based silver nanoparticles and their antibacterial activity. *Carbohydr Res* **2009**, *344*, 2375-2382, <https://doi.org/10.1016/j.carres.2009.09.001>.

## 6. ACKNOWLEDGEMENTS

The authors are thankful to the Ministry of Higher Education Malaysia for financial assistant in Research Acculturation Grant Scheme (RAGS) vote no. 57117, Mybrain15 for scholarship sponsor and Universiti Malaysia Terengganu for providing the facilities.



© 2020 by the authors. This article is an open access article distributed under the terms and conditions of the Creative Commons Attribution (CC BY) license (<http://creativecommons.org/licenses/by/4.0/>).